Conditioned medium derived from human amniotic stem cells delays H_2O_2-induced premature senescence in human dermal fibroblasts

CHANGWEI PAN[1], HONGXIN LANG[1], TAO ZHANG[1], RUI WANG[1], XUEWEN LIN[1], PING SHI[2], FENG ZHAO[1] and XINING PANG[1]

[1]Department of Stem Cells and Regenerative Medicine, Key Laboratory of Cell Biology, Ministry of Public Health of China, China Medical University, Shenyang, Liaoning 110013; [2]Shenyang Amnion Biological Engineering Technology Research and Development Center Limited Company, Shenyang, Liaoning 110629, P.R. China

Received November 14, 2018; Accepted July 8, 2019

DOI: 10.3892/ijmm.2019.4346

Abstract. Stem cells derived from human amniotic membrane (hAM) are promising targets in regenerative medicine. A previous study focused on human amniotic stem cells in skin wound and scar-free healing. The present study aimed to investigate whether hydrogen peroxide (H_2O_2)-induced senescence of human dermal fibroblasts (hDFs) was influenced by the anti-aging effect of conditioned medium (CdM) derived from human amniotic stem cells. First, the biological function of two types of amniotic stem cells, namely human amniotic epithelial cells (hAECs) and human amniotic mesenchymal stem cells (hAMSCs), on hDFs was compared. The results of cell proliferation and wound healing assays showed that CdM promoted cell proliferation and migration. In addition, CdM from hAECs and hAMSCs significantly promoted proliferation of senescent hDFs induced by H_2O_2. These results indicated that CdM protects cells from damage caused by H_2O_2. Treatment with CdM decreased senescence-associated β-galactosidase activity and improved the entry of proliferating cells into the S phase. Simultaneously, it was found that CdM increased the activity of superoxide dismutase and catalase and decreased malondialdehyde by reducing H_2O_2-induced intracellular reactive oxygen species production. It was found that CdM downregulated H_2O_2-stimulated 8-hydroxydeoxyguanosine and γ-H2AX levels and decreased the expression of the senescence-associated proteins p21 and p16. In conclusion, the findings indicated that the paracrine effects derived from human amniotic stem cells aided delaying oxidative stress-induced premature senescence.

Correspondence to: Professor Xining Pang or Dr Feng Zhao, Department of Stem Cells and Regenerative Medicine, Key Laboratory of Cell Biology, Ministry of Public Health of China, China Medical University, 77 Puhe Street, Shenbei, Shenyang, Liaoning 110013, P.R. China
E-mail: pangxining@126.com
E-mail: unicorn.zhao@163.com

Key words: human amniotic epithelial cells, human amniotic mesenchymal stem cells, human dermal fibroblasts, hydrogen peroxide, senescence

Introduction

Human skin, the largest organ of the human body, plays an important role in biological function and exerts critical effects as a front-line defense system against various harmful substances in the environment, including reactive oxygen species (ROS) and UV-radiation, that can cause premature skin aging (1). When skin is aged, it becomes looser, more fragile and wrinkled (2,3). Cell senescence is caused by multiple mechanisms, such as cell growth arrest, increased activity of senescence-associated-β-galactosidase (SA-β-gal), cell cycle arrest and upregulation of cell cycle inhibitors, including p21 and p16 (4-7).

Skin consists of epidermal, dermal and subcutaneous tissues, among which fibroblasts, a major cellular component of the dermal tissue, play an important role in restoring tissue after dermis injury (8). ROS include the superoxide anion, hydroxyl radicals and hydrogen peroxide (H_2O_2). According to the free radical damage theory of senescence, premature senescence of human dermal fibroblasts (hDFs) can be induced by a sublethal dose of H_2O_2 (9). Excessive free radicals can attack cellular components, causing peroxidation of lipids, proteins and nucleic acids (10). Despite the existence of an intracellular antioxidant enzyme system, excessive ROS can exceed the clearance limit of antioxidant enzymes, leading to an intracellular imbalance in oxidation and antioxidant activities, and ultimately resulting in cell apoptosis or senescence (11-13). Superoxide dismutase (SOD) and catalase (CAT) are key intracellular antioxidant enzymes that contribute to the enzymolysis of superoxide anions and H_2O_2 into water and oxygen, thereby delaying cell senescence (14). Mitochondrial DNA has a bare ring structure that lacks a protein protection and damage repair systems, which makes it more susceptible to damage (15). As a result, it may directly affect the electron transfer process, causing mitochondrial dysfunction resulting

in increased leakage of ROS, a byproduct of the respiratory chain and eventually, sustained damage occurs (16).

Human amniotic epithelial cells (hAECs) and human amniotic mesenchymal stem cells (hAMSCs) can be isolated from the human amniotic membrane (hAM) and these cells have low immunogenicity and secrete numerous growth factors (17). Various reports have shown that hAM, hAECs and hAMSCs are used to treat wounds, burn lesions and chronic ulcers (18,19). However, the purpose of the current study was to compare the therapeutic potency of conditioned medium (CdM) derived from hAM cells (hAMCs) on delaying senescence in H_2O_2-induced premature senescence of hDFs and to provide an experimental basis for the application of hAM cells in the beauty industry.

Materials and methods

Isolation and culture of hDFs. Primary hDFs were derived from the healthy dermis of three adult donors (age, 20-30 years; all male) undergoing surgical debridement. All samples were negative for human immunodeficiency virus-1, hepatitis B and hepatitis C virus infection. All samples were obtained from August to October 2017 at the Shengjing Hospital of China Medical University and written informed consent was obtained from all patients. The experiments of the present study were approved by the Ethics Committee of the Shengjing Hospital of China Medical University (Shengyang, China). Fresh healthy skin tissue was washed twice with PBS containing 100 U/ml penicillin and 100 U/ml streptomycin in a culture dish, and subcutaneous fat and connective tissue was removed with scissors. The skin slice was then cut into 1x1 cm pieces and placed in 15 ml centrifuge tubes, followed by the addition of Dispase II enzyme solution (2 mg/ml; Roche Diagnostics) before incubation at 4˚C overnight. On the second day, the epidermis was removed with tweezers. The dermis was cleaned twice with sterile PBS, cut into 5x5 mm pieces, moved into T25 culture flasks and were incubated at 37˚C for 2 h to facilitate tissue adhesion. Following incubation, 4 ml high glucose DMEM (HyClone; GE Healthcare Life Sciences) containing 10% fetal bovine serum (FBS; referred to as hDF; HyClone; GE Healthcare Life Sciences) with penicillin (100 U/ml) and streptomycin (100 U/ml) was added and plates were incubated at 37˚C with 5% CO_2. At 80-90% confluence at the bottom of the flask, cells were subcultured and the cell passage (P) was recorded as P0. hDFs at P3-P5 were used for subsequent assays.

hAECs. Human amnions were obtained from healthy patients undergoing caesarean sections at full term (39-40 weeks). The procedures were approved by the Ethics Committee of the First Affiliated Hospital of China Medical University. Written informed consent was obtained from all patients prior to participation. Human amnion samples were obtained from 6 females (age, 25-30 years) between December 2016 and April 2018. Amnion samples washed three times with PBS to remove blood. Then, amnions were cut into 5x5 cm pieces, trypsin (0.25%; Gibco; Thermo Fisher Scientific, Inc.) was added and samples were digested for 20 min at 37˚C. The digestive liquid was collected and added to DMEM/F12 (HyClone; GE Healthcare Life Sciences) containing 10% FBS to terminate digestion. The steps were repeated three times and subsequently, the obtained single cell suspension was centrifuged at 140 x g for 10 min at room temperature and the supernatant was removed. The precipitate was suspended in complete hAEC medium, containing DMEM/F12 containing 10% FBS, 1% nonessential amino acids, 1% L-glutamine and 10 ng/ml EGF (all Thermo Fisher Scientific, Inc.). Cells were inoculated at $2.5x10^9$ cells/l in 25 cm^2 culture flasks before incubation in saturated humidity at 37˚C with 5% CO_2. After 24 h, medium was replaced and P0 was set when the cells had completely covered bottom of the flask. hAECs at P2-P3 were used for subsequent assays.

hAMSCs. Tissues after the isolation of hAECs were incubated in 1 mg/ml collagenase IV (Sigma-Aldrich; Merck KGaA) at 37˚C for 30 min. FBS (10%) was added to terminate digestion and the supernatant was filtered using a cell strainer (200 μm) before centrifugation at 140 x g for 10 min at room temperature. Cells were then cultured in complete hAMSC medium, containing DMEM/F12 containing 100 U/ml penicillin, 100 U/ml streptomycin and 10% FBS, and medium was replaced every 48 h. P0 was set when cells completely covered the bottom of the flask. hAMSCs at P3-P6 were used in subsequent experiments.

Flow cytometric analysis. P2 hAECs and P3 hAMSCs were collected, washed with PBS, digested with trypsin (0.25%) at 37˚C with 5% CO_2 for 2 min and resuspended in 100 μl cold PBS at 10^6 cells/tube. Each samples was mixed with 5 μl phycoerythrin-conjugated antibody against CD31 (cat. no. 303105), CD34 (cat no. 343505), CD45 (cat. no. 368509), CD90 (cat. no. 32810), CD105 (cat. no. 323205), CD117 (cat. no. 313204), human leukocyte antigen (HLA)-DR (cat. no. 307605) or stage-specific embryonic antigen-4 (SSEA-4; cat. no. 330405; all BioLegend, Inc.) PE-conjugated nonspecific mouse IgG was used as isotype control (cat. no. 40011; BioLegend, Inc.). Samples were then incubated at 4˚C for 30 min in the dark. After two washes with cold PBS, the stem cell surface markers were detected using FACSDiva 6.2 (BD Biosciences); 10,000 cells were used for each test.

Cell immunofluorescence staining. P3 hDFs were seeded in a 12-well plate with a glass slide at $4x10^4$ cells/well. At 80% confluence, culture medium was discarded and cells were fixed with 4% paraformaldehyde at room temperature for 30 min and washed with PBS twice. Afterwards, Triton X-100 (0.1% in PBS) was allowed to permeate the cells for 10 min at room temperature. Then, cells were blocked with bovine serum albumin (5%; Beijing Solarbio Science & Technology Co., Ltd.) for 30 min at room temperature. Vimentin primary antibody (rabbit anti-human; cat. no. abp52697; 1:200; Abbkine Scientific, Co., Ltd.) was added and samples were incubated at 4˚C overnight. Cells were washed three times with PBS on the second day, followed by addition of the secondary fluorescent antibody (Alexa 488; donkey anti-rabbit; cat. no. A-11034; 1:200; Thermo Fisher Scientific, Inc.) and incubation at room temperature for 1 h in the dark. Cell nuclei were stained with DAPI diluted in PBS (1:1,000) for 5 min at room temperature, followed by dilution with PBS (1:1,000). Images were recorded with an inverted fluorescence microscope (magnification, x100).

Preparation of CdM. To obtain CdM, hAECs or hAMSCs were cultured in complete hAEC or hAMSC medium until 60-70% confluence. After two washes with PBS, cells were cultured in 10% FBS in high glucose DMEM for 48 h. Cells were then centrifuged at 1,000 x g for 5 min at room temperature; supernatants were labeled CdM-hAEC or CdM-hAMSC and mixed with fresh growth hDF medium (1:1) to be labeled as CdM1/2-hAEC or CdM1/2-hAMSC. CdM was stored in small sized tubes at -80˚C.

H_2O_2 and CdM treatments. For establishment of the premature senescence model, hDFs were treated with 50, 100, 200 and 400 μM H_2O_2 (in 10% FBS in high glucose DMEM) at 37˚C with 5% CO_2 for 1 or 2 h. Cells were then washed with serum-free high glucose DMEM twice to remove residual H_2O_2 (20,21) and cultured in high glucose DMEM with 10% FBS for 4 days; growth medium changed every 48 h. In the CdM treatment group, H_2O_2-treated cells (200 μM, 1 h) were washed with serum free medium and incubated with CdM for 4 days. To ensure sufficient nutrients were available, CdM was changed every 24 h.

Cell proliferation assay. hDFs were seeded in 96-well plates at $5x10^3$ cells/well and incubated in growth medium for 24 h for adherence. Then, H_2O_2-treated cells (50, 100, 200 and 400 μM, for 1 or 2 h) and cells of the control group were continued to be cultured in growth medium for 4 or 7 days to test the sustained effect of H_2O_2 on cell proliferation, while cells in the CdM group were incubated with 200 μl CdM for 4 days. A cell proliferation assay was performed using CellTiter 96® AQueous One Solution Cell Proliferation assay (Promega Corporation). According to the manufacturer's instructions, 100 μl serum-free high glucose DMEM from each plate was mixed with 20 μl MTS and incubated for 1 h at 37˚C with 5% CO_2. The OD was measured at 490 nm. Cell viability was assessed according to the following formula: Viability (%)=OD of experimental group/OD of control group x100.

Cell viability using fluorescein diacetate (FDA) staining. FDA (Sigma-Aldrich; Merck KGaA) was used to visually present living cells. According to the manufacturer's instructions, $5x10^4$ cells/well were seeded in 12-well plates and incubated in growth medium for 24 h for adherence. Then, cells of the control and H_2O_2 group were continued to grow in growth medium, while cells in the CdM group were incubated with 1 ml CdM for further 4 days. Then, hDFs were washed twice with PBS before incubation at 37˚C with 5% CO_2 for 15 min in FDA solution (10 μg/ml; in acetone). After that, cells were washed twice with PBS and cells were observed and five randomly chosen fields were taken using an inverted fluorescence microscope (magnification, x100).

Scratch wound closure assay. A scratch test was used to analyze the migration abilities of hDFs treated with CdM. P3 hDFs were seeded in a 6-well plate at $5x10^4$ cells/well. At 80-90% confluence, scratches with 0.4-0.5 mm width were inflicted using sterile suction tips. Then, each well was washed twice with PBS to remove loose cell fragments. After that cells incubated with 10% FBS in high glucose DMEM were labeled as the control. Cells were cultured in the respective CdM were labeled as CdM-hAEC and CdM-hAMSC groups. Cell migration was observed using an inverted microscope (magnification, x20) after 0, 12 and 24 h. Results were expressed as: Migration (%) = [Wound area (initial)-Wound area (final)]/Wound area (initial)x100.

SA-β-gal staining. H_2O_2-treated hDFs were seeded in 12-well plates at $5x10^4$ cells/well and incubated in growth medium for 24 h for adherence. Then, cells of the control and H_2O_2 group were continued to grow in growth medium, while cells in the CdM group were incubated with 1 ml CdM for further 4 days. Cells were washed with PBS, cells were stained using the SA-β-gal staining kit (Beyotime Institute of Biotechnology) according to the manufacturer's instructions. Briefly, cells were immobilized at room temperature with β-gal fixative for 15 min, followed by three washes with PBS for 3 min and 500 μl staining working solution were added before cells were incubated overnight at 37˚C in a CO_2-free incubator. Pictures from five consecutive fields of view were randomly selected; pictures were taken with inverted microscope (magnification, x20). The percentage of SA-β-gal-positive cells was calculated as: SA-β-gal positive cells/total cells x100.

Cell cycle. Cell cycle distribution was detected using flow cytometry with PI staining. Briefly, H_2O_2-treated hDFs were seeded in 6-well plates at $1.2x10^5$ cells/well. Cells of the control and H_2O_2 group were continued to be cultured in hDF, while cells in the CdM group were incubated with 2 ml CdM for further 4 days. Then, cells were suspended, washed with PBS and fixed in 70% ethanol at 4˚C for 24 h. Cells were then suspended in 300 μl dyeing solution (500 μl buffer containing 10 μl RNase A and 25 μl PI) and incubated at 37˚C for 30 min in the dark. A total of $1x10^4$ cells/sample were subjected to cell cycle analysis using FACS with the FACSDiva 6.2 (BD Biosciences).

Detection of SOD, CAT and malondialdehyde (MDA). To evaluate the effect of CdM on antioxidant enzyme activity after H_2O_2 treatment, the levels of intracellular total SOD (cat. no. A001-3-2), MDA (cat. no. A003-4-1) and CAT (cat. no. A007-1-1) in the supernatant of cultured cells were detected using corresponding kits (all Nanjing Jiancheng Bioengineering Institute) according to the manufacturer's instructions. In brief, cells ($1.2x10^5$) were seeded in 6-well plates, control and H_2O_2 group were continued to be cultured in hDF, while cells in the CdM group were incubated with 2 ml CdM for further 4 days. Then, cells were washed twice with PBS and 200 μl RIPA buffer (Beyotime Institute of Biotechnology) was added to each well of a 6-well plate to lyse the cells on ice for 10 min. Then, cells were collected and centrifuged at 3,000 x g for 10 min at 4˚C. The OD was detected at 450 nm using 20 μl supernatant for SOD, at 530 nm using 100 μl for MDA and at 405 nm using 100 μl for CAT. A total of 25 μl supernatant was used for protein content determination (BCA Protein Assay kit; Tiangen Biotech Co., Ltd.). Enzyme activity was calculated based on the manufacturer's instructions: SOD activity (U/mg protein)=inhibition ratio/50% x reaction system/dilution multiple/protein concentration (mg/ml). MDA content (nmol/mg protein)=OD value-blank OD value/standard OD value-blank OD value x

standard concentration (10 nmol/ml)/protein concentration (mg/ml). CAT activity (U/ml) = (control OD value-measured OD value) x 235.65 x 1/(60 x sampling quantity) x dilution multiple before testing.

Detection of ROS levels. Intracellular ROS levels in hDFs were measured with using the Reactive Oxygen Species Assay kit (Beyotime Institute of Biotechnology). According to the manufacturer's instructions, cells were suspended in 10 μmol/l 2',7'-dichlorodihydrofluorescein diacetate (DCFH-DA; in serum-free medium) and incubated for 20 min at 37˚C with 5% CO_2; cells were mixed every 5 min during incubation. After three washes with serum-free medium, fluorescence images were taken with an inverted fluorescence microscope (magnification, x100).

Reverse transcription-quantitative (RT-q)PCR analysis. Total RNA was isolated from hDFs after exposure to H_2O_2 for 1 h and co-culture with CdM for 4 days using TRIzol® reagent (Invitrogen; Thermo Fisher Scientific, Inc.). RNA with an A_{260}/A_{280} of 1.8-2.0 was considered pure and used for subsequent assays. cDNA was synthesized from 1 μg total RNA using GoScript™ RT kit (cat. no. A2791; Promega Corporation); the following conditions were applied: 70˚C for 5 min followed by 25˚C for 5 min, 42˚C for 60 min and 70˚C for 15 min. qPCR was performed using the SYBR Premix Ex Taq™ II kit (Takara Bio, Inc.) and the thermocycling conditions were as follows: 95˚C for 30 sec, followed by 40 cycles of 95˚C for 5 sec and 60˚C for 34 sec. GAPDH was used as internal control. Results were calculated using the $2^{-\Delta\Delta Cq}$ method (19). Each sample was analyzed in triplicate. Primer sequences were as follows: p21, forward, 5'-CTGGAGACT CTCAGGGTCGAA-3' and reverse, 5'-CCAGGACTGCAG GCTTCCT-3'; GAPDH, forward, 5'-ACCCACTCCTCCACC TTTGAC-3' and reverse, 5'-GTCCACCACCCTGTTGCTG-3'.

Western blotting. The control, H_2O_2 and CdM groups were washed three times with cold PBS and lysed on ice with RIPA buffer containing a protease inhibitor (Roche Diagnostics). The BCA Protein Assay kit was used for protein quantification. Samples were separated on SDS-PAGE gels and transferred to polyvinylidene fluoride membranes. Membranes were blocked at room temperature for 2 h with 5% non-fat milk and then incubated with primary antibodies: p21 and H2AX (cat. nos. 10355-1-AP and 10856-1-AP, respectively; 1:1,000; ProteinTech Group, Inc.), p16 (cat. no. WL01418; 1:1,000; Wanleibio, Co., Ltd.), γ-H2AX (22) and β-actin (cat. nos. ab2893 and ab8226, respectively; 1:1,000; Abcam) at 4˚C overnight. Membranes were then incubated with an HRP-conjugated goat anti-rabbit IgG (cat. no. SA00001-2; 1:2,500) or goat anti-mouse IgG (cat. no. SA00001-1; 1:2,500; all ProteinTech Group, Inc.) for 1 h at room temperature. Immunoreactive bands were visualized using the SuperSignal West Pico Chemiluminescent substrate (Pierce; Thermo Fisher Scientific, Inc.) using LAS-3000 mini (Fuji). β-actin was used as an internal control. The bands were analyzed by using Image J software version 1.48 (National Institutes of Health).

ELISA. 8-hydroxydeoxyguanosine (8-OHdG) was detected as a marker of DNA damage using the 8-OHdG ELISA kit (cat. no. BYE10099; Shanghai Bangyi Biotechnology). The control, H_2O_2 group and CdM groups were washed twice with PBS followed by the addition of 100 μl RIPA buffer (Beyotime Institute of Biotechnology) and centrifugation at 3,000 x g for 20 min at 4˚C. A total of 40 μl sample diluent provided with the kit and 10 μl sample were added to the enzyme-labeled coating plate before sealing and incubation at 37˚C for 30 min. According to the manufacturer's instructions, the OD at 450 nm was determined.

Statistical analysis. Data are presented as the mean ± standard deviation. All assays were repeated three times. Comparison between two groups was performed using an independent sample t-test or for multiple groups one-way ANOVA followed by Tukey's test. All statistical analyses were performed with Graph Pad Prism 5.0 (GraphPad Software, Inc.) and SPSS 19.0 (IBM Corp.). $P<0.05$ was considered to indicate statistical significant difference.

Results

Characterization of hDFs, hAECs and hAMSCs. hDFs were spindle shaped and showed typical fibroblast morphology (Fig. 1A). Immunofluorescence analysis demonstrated that the cells were positive for the hDF surface marker vimentin (Fig. 1B) (23). hAECs and hAMSCs were isolated from hAMs and hAECs exhibited cobblestone-like morphology (Fig. 1A), the typical morphology of hAECs (19). The morphology of hAMSCs was similar to that of fibroblasts, as fibrous cell morphology was observed in the plastic plates (Fig. 1A). Flow cytometry was used to detect the expression of surface markers on hAECs and hAMSCs. hAECs and hAMSCs expressed CD90 and CD105, but did not express CD31, CD34, CD45 or the hematopoietic progenitor cell marker CD117. In addition, SSEA-4 was expressed by hAMSCs but not by hAECs, and immune-related marker HLA-DR was not expressed by either cells (Fig. 1C and D). These results were consistent with observations from previous reports (24,25).

CdM alleviated the inhibitory effect of H_2O_2 on hDFs growth. To evaluate effects of H_2O_2 on hDFs, 50, 100, 200 and 400 μM H_2O_2 was used to treat hDFs for 1 or 2 h, followed by 4 and 7 day culture. Based on MTS assay results, after 1 and 2 h H_2O_2 treatment at varying concentrations, the cell viability was significantly reduced compared with the control ($P<0.05$; Fig. 2A and B). After culturing for 4 days following 1 h treatment, cell viability was 49.30±1.57, 35.87±1.20, 24.30±3.46 and 18.71±1.31% in the 50, 100, 200 and 400 μM groups, respectively. Following 7 days of culture after 1 h H_2O_2 treatment, cell viability was 18.21±1.91% in the 50 μM group, 15.23±1.56% in the 100 μM group, 13.78±0.89% in the 200 μM group and 13.50±1.15% in the 400 μM group. After H_2O_2 treatment for 2 h followed by 7 days of culturing, for 50, 100, 200 and 400 μM H_2O_2 groups the cell viability was 51.14±2.01, 41.94±0.88, 17.49±1.12, and 4.21±0.95%, respectively. Following seven-day culture, cell viability was 38.41±3.24, 4.22±1.94, 0.44±0.34 and 0.38±0.31% for the 50, 100, 200 and 400 μM groups, respectively. The results revealed that H_2O_2 treatment for 1 h and 2 h caused damage even after prolonged periods of culturing.

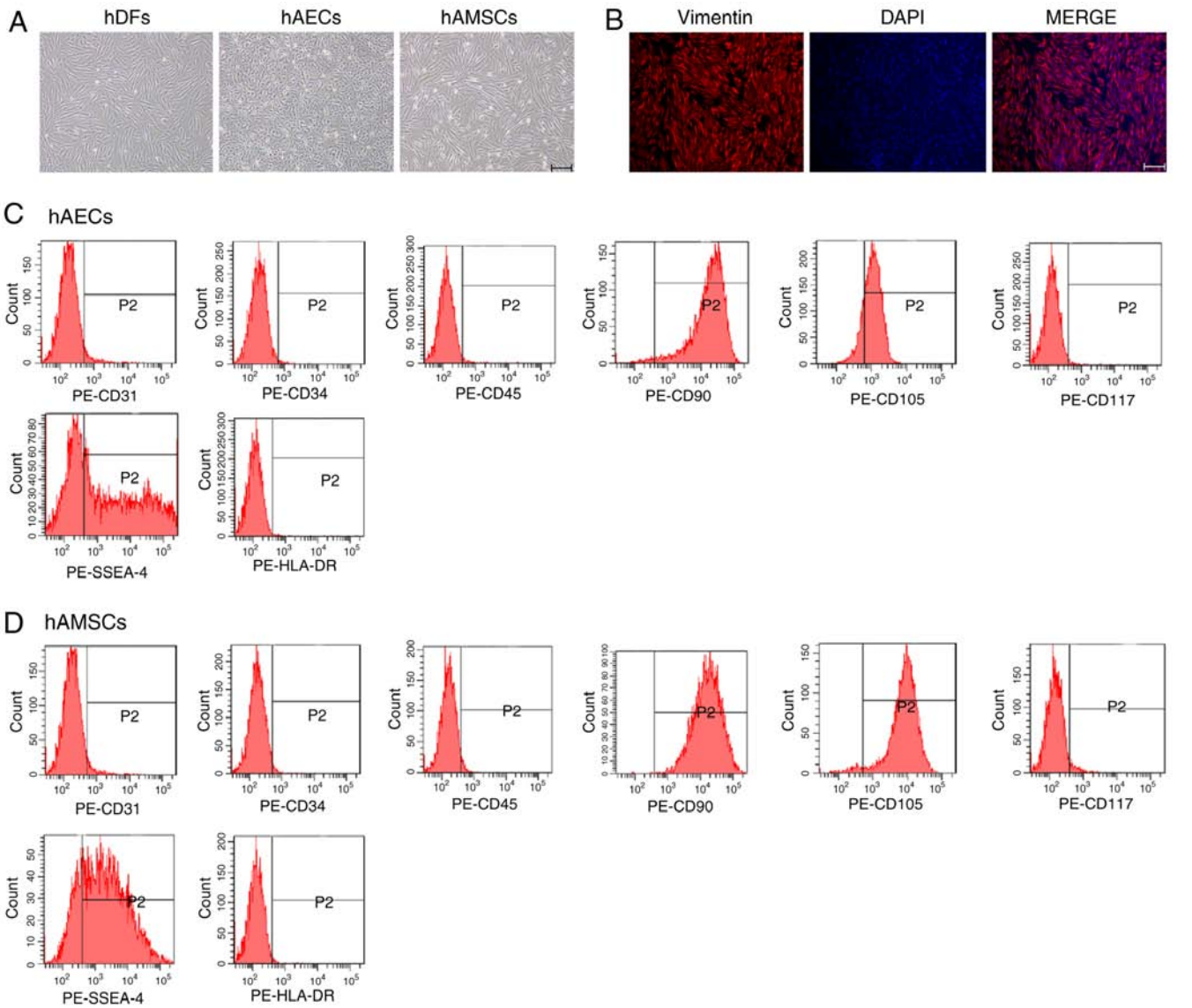

Figure 1. Characterization of hDFs, hAECs and hAMSCs. (A) Morphology of hDFs, hAECs and hAMSCs at passage 2. Scale bar, 200 μm. (B) Vimentin expression in hDFs using immunofluorescence. Scale bar, 100 μm. Cell markers determined by flow cytometry for (C) hAECs and (D) hAMSCs. hDF, human dermal fibroblast; hAEC, human amniotic epithelial cell; hAMSC, human amniotic mesenchymal stem cell; HLA, human leukocyte antigen; SSEA-4, stage-specific embryonic antigen-4.

To study the effect of CdM derived from hAM cells on the proliferation of hDFs, cells were cultured with CdM1/2 or CdM from hAMSCs or hAECs for 1 day. Results indicated that the CdM1/2-hAMSC group exhibited significantly greater cell proliferation compared with the control group at the 1 and 2 day measurements ($P<0.05$; Fig. 2C). In the 2 day experiments, the determined OD values for CdM1/2-hAEC, CdM-hAEC, CdM1/2-hAMSC and CdM-hAMSC were 0.70±0.02, 0.78±0.04, 0.75±0.04 and 0.71±0.03, respectively, all significantly increased compared with the control group (0.58±0.04; $P<0.05$; Fig. 2C). In the 3 day measurement, OD values of CdM-hAEC and CdM-hAMSC were significantly higher compared with the control ($P<0.05$; Fig. 2C), while the 50% CdM showed no significant improvement compared with the control. To explore whether CdM alleviated the damage caused by H_2O_2, two concentrations of CdM were tested as medium for cells following 200 μM H_2O_2 exposure for 1 h. The results showed that the effect in the 200 μM H_2O_2+CdM-hAEC group was significantly improved compared with the 200 μM H_2O_2+CdM1/2-hAEC group and cell proliferation was significantly promoted compared with the 200 μM H_2O_2 control group ($P<0.05$; Fig. 2D). In comparison with the 200 μM H_2O_2 group, cell proliferation was significantly promoted in the 200 μM H_2O_2+CdM-hAMSC group ($P<0.05$; Fig. 2E), while 1/2CdM-hAMSC did not exhibit a significant improvement.

Effect of CdM on living cell density is assessed using FDA probes. FDA staining was used to trace density changes in living cells to verify results of proliferation experiments and account for influences of cells with poor viability. CdM was found to promote proliferation of hDFs after H_2O_2 treatment (Fig. 3A). Fluorescence images revealed that the cell density was markedly higher in the 200 μM H_2O_2+CdM-hAEC and the 200 μM H_2O_2+CdM-hAMSC group compared with the 200 μM H_2O_2 group. The strongest effect was observed for the 200 μM H_2O_2+CdM-hAEC group. These results were consistent with cell proliferation data.

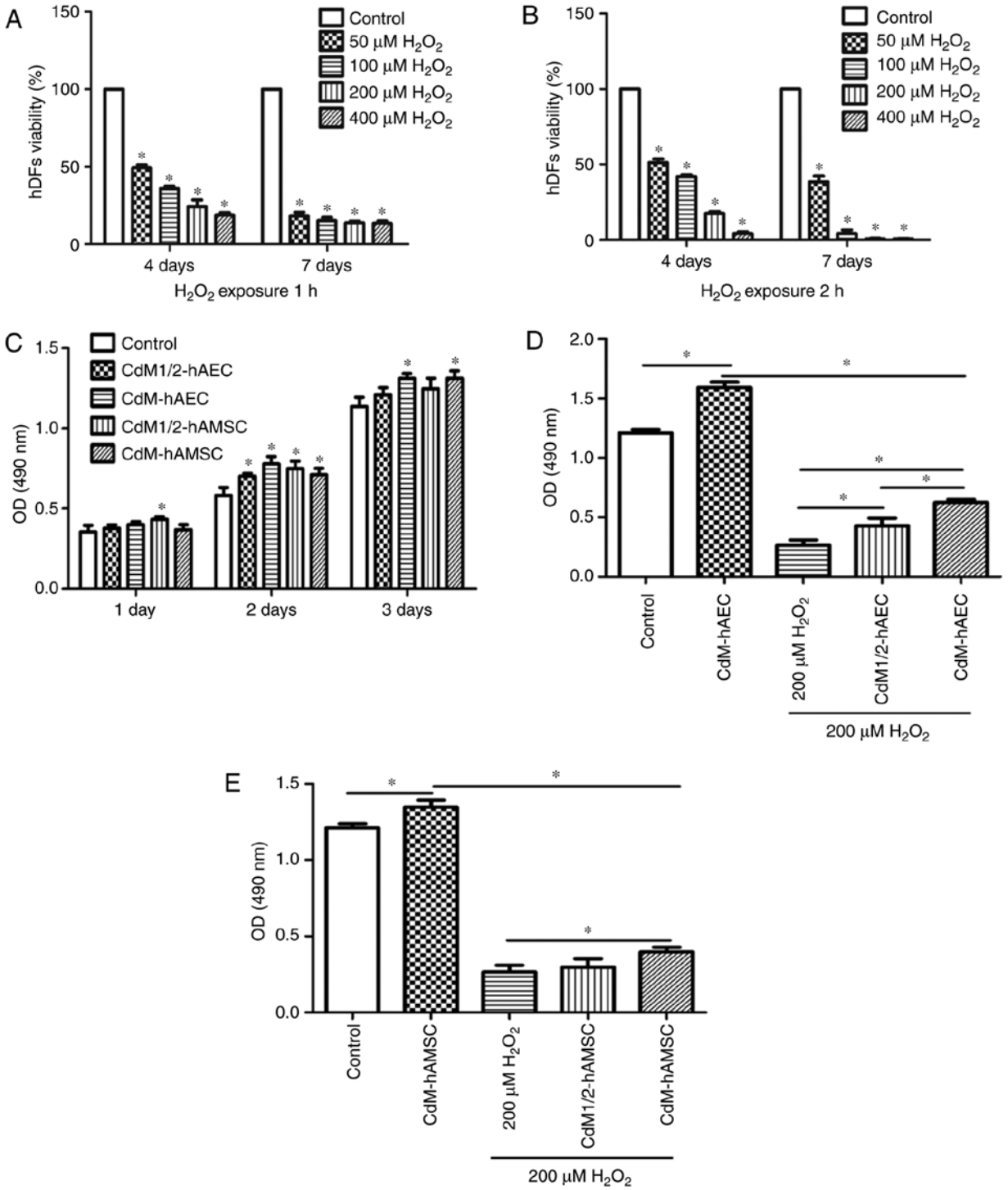

Figure 2. H_2O_2 inhibits hDFs growth and CdM affects proliferation in H_2O_2-treated hDFs. Cell viability at 4 and 7 days after exposure to H_2O_2 for (A) 1 and (B) 2 h at varying concentrations determined by MTS assay (n=3). *P<0.05 vs. control. (C) Effect of CdMs from hAECs and hAMSCs on hDF proliferation. *P<0.05 vs. control. hDF proliferation of cells treated with 200 μM H_2O_2 for 1 h followed by incubation with (D) CdM1/2-hAEC and CdM-hAEC, and (E) CdM1/2-hAMSC and CdM-hAMSC for 4 days. *P<0.05. H_2O_2, hydrogen peroxide; CdM, conditioned medium; hDF, human dermal fibroblast; hAEC, human amniotic epithelial cell; hAMSC, human amniotic mesenchymal stem cell; CdM1/2, 50% CdM.

CdM enhances the migration ability of hDFs. To examine whether CdM-hAEC and CdM-hAMSC exhibited biological effects relevant to hDF migration, a scratch assay was conducted. hDFs were imaged after 12 and 24 h in CdM-hAEC and CdM-hAMSC and results are shown in Fig. 3B. The migration into the wound was accelerated compared with that of the control group. After 12 h of culture, the migration percentage in the CdM-hAMSC group was significantly higher compared with the control. After 24 h of culture, the migration percentage in the CdM-hAEC and the CdM-hAMSC groups were significantly higher compared with the control (P<0.05; Fig. 3C) and the observed effect was superior compared with the CdM-hAEC group.

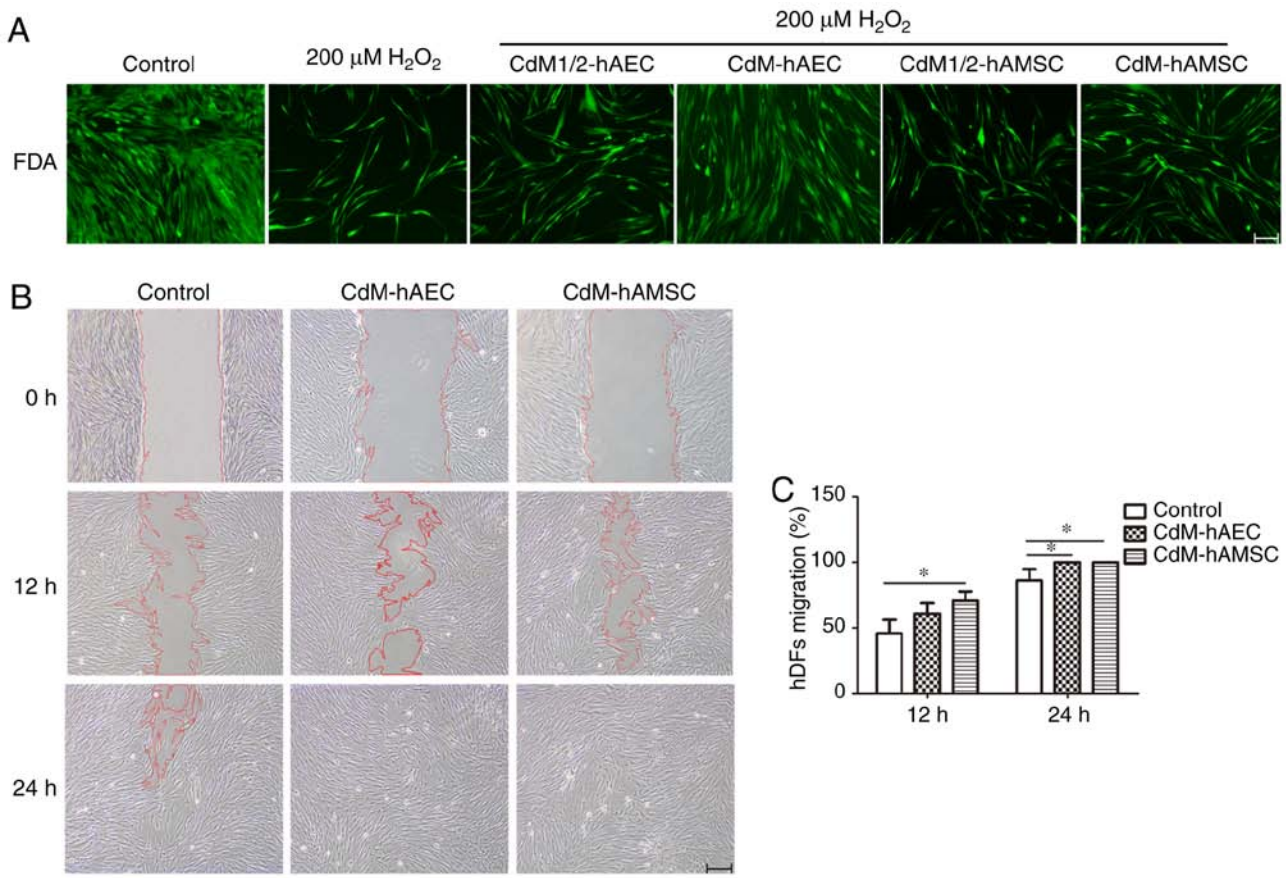

Figure 3. Effect of CdM on hDF proliferation and migration. (A) hDFs were treated with 200 μM H_2O_2 for 1 h and cultured in CdM1/2-hAEC, CdM-hAEC, CdM1/2-hAMSC or CdM-hAMSC for 4 days. Cell density was observed in FDA stained fluorescence images. Scale bar, 50 μm. (B) Migration of hDFs following scratch at 0, 12 and 24 h of culture in CdM-hAEC or CdM-hAMSC. Scale bar, 200 μm. (C) Rate of wound healing. *P<0.05. H_2O_2, hydrogen peroxide; CdM, conditioned medium; hDF, human dermal fibroblast; hAEC, human amniotic epithelial cell; hAMSC, human amniotic mesenchymal stem cell; CdM1/2, 50% CdM; FDA, fluorescein diacetate.

CdM from hAECs affects cell distribution in the S phase after H_2O_2 exposure. Cell cycle distribution was determined by flow cytometry. The results showed that the percentage of cells in the S phase significantly decreased in the 200 μM H_2O_2 group compared with the control (P<0.05; Fig. 4A and B). CdM-hAEC significantly increased the percentage of cells in the S phase compared with the 200 μM H_2O_2 group (P<0.05); effects of CdM-hAMSC were not significant. No significant changes in the G0/G1 or the G2/M phases were observed.

CdM from hAECs and hAMSCs reduce H_2O_2 induced HDFs senescence. A senescence-specific SA-β-gal staining assay was conducted to observe hDFs treated with H_2O_2. The results showed that the number of positive cells was significantly increased in the 200 μM H_2O_2 group compared with the control group (67.0±4.87 vs. 1.0±0.16%; P<0.05; Fig. 4C and D). After treatment with 200 μM H_2O_2 for 1 h and culturing in CdM-hAEC or CdM-hAMSC for 4 days, the percentage of positive cells were 41.75±2.49 and 44.43±3.20%, respectively (Fig. 4C and D), both significantly decreased compared with the 200 μM H_2O_2 group (P<0.05).

CdM from hAECs and hAMSCs alleviates oxidative stress induced by H_2O_2. The generation of ROS was determined using the ROS-specific fluorescent dye DCFH-DA. The results showed that treatment of hDFs with H_2O_2 for 1 h, ROS levels were significantly higher compared with the control group (P<0.05; Fig. 4E and F). In addition, using CdM-hAEC and CdM-hAMSC as culture medium after H_2O_2 exposure significantly reduced the level of ROS compared with the 200 μM H_2O_2 group (P<0.05; Fig. 4E and F). Furthermore, ELISA results showed that for hDFs treated with H_2O_2 for 1 h, activities of SOD and CAT were significantly decreased and the concentration of MDA was significantly increased compared with the control group (P<0.05; Table I).

Next, 8-OHdG and γ-H2AX levels were assessed, reflecting the extent of DNA damage caused by oxidation (26,27). H_2O_2 treatment significantly increased 8-OHdG levels compared with the control group (P<0.05; Fig. 5A). Culturing in CdM-hAEC and CdM-hAMSC after H_2O_2 treatment significantly decreased the 8-OHdG levels in hDFs detected by ELISA compared with the 200 μM H_2O_2 group (P<0.05; Fig. 5A). Levels of γ-H2AX and H2AX were measured by western blot to analyze the therapeutic efficacy of CdM after H_2O_2 treatment. Results showed that γ-H2AX levels were significantly upregulated after H_2O_2 treatment compared with the control. For hDFs cultured in CdM-hAEC and CdM-hAMSC after peroxide challenge, γ-H2AX levels were significantly decreased and H2AX levels were markedly

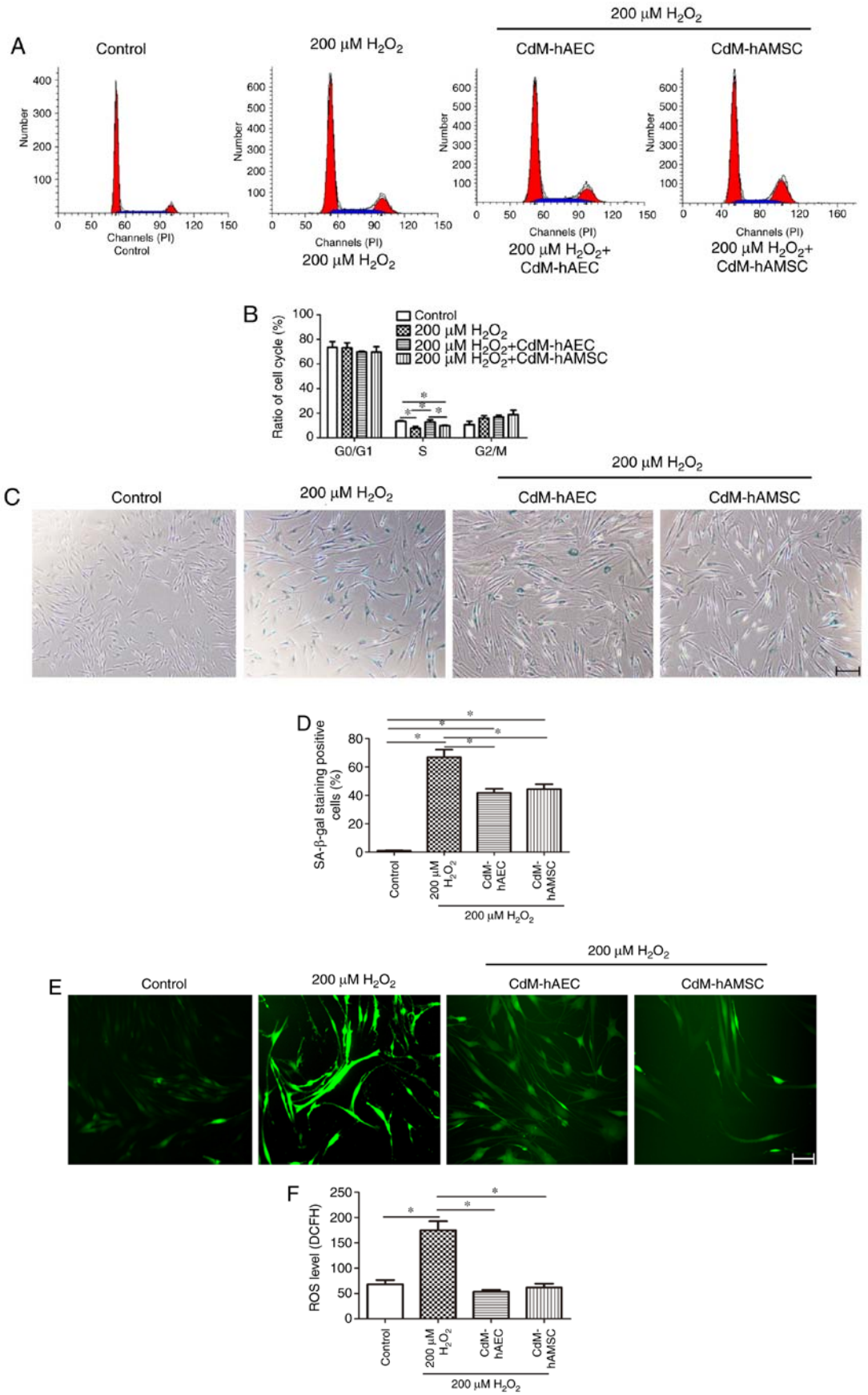

Figure 4. Treatment with CdM alleviate H_2O_2-induced premature senescence. hDFs were treated with 200 μM H_2O_2 for 1 h and cultured in CdM-hAEC or CdM-hAMSC for 4 days. (A) Flow cytometric analysis of the cell cycle and (B) determined cell cycle distribution of hDFs. (C) Representative images for SA-β-gal staining (blue, cells positive for senescence). Scale bar, 200 μm. (D) Quantification of SA-β-gal-positive cells. (E) ROS levels determined using DCFH fluorescence. Scale bar, 50 μm. (F) Quantified ROS fluorescence intensity. Data are presented as the mean ± standard deviation (n=3). $^*P<0.05$. H_2O_2, hydrogen peroxide; CdM, conditioned medium; hDF, human dermal fibroblast; hAEC, human amniotic epithelial cell; hAMSC, human amniotic mesenchymal stem cell; SA-β-gal, senescence-associated-β- galactosidase; ROS, reactive oxygen species.

Table I. Levels of total-SOD, CAT and MDA in hDFs.

Group	Total-SOD (U/mg protein)	CAT (U/ml)	MDA (nmol/mg protein)
Control	78.4±2.5	1.29±0.07	18.2±2.2
200 μM H_2O_2	32.7±2.4[a]	0.15±0.05[a]	101.0±1.1[a]
200 μM H_2O_2+CdM-hAEC	82.1±8.4[b]	1.62±0.11[a,b]	8.5±1.8[b]
200 μM H_2O_2+CdM-hAMSC	43.1±2.9[a,c]	0.60±0.08[a-c]	44.2±8.0[a-c]

Data are presented as the mean ± standard deviation (n=3). [a]P<0.05 vs. control; [b]P<0.05 vs. 200 μM H_2O_2; [c]P<0.05 vs. 200 μM H_2O_2+CdM-hAEC. H_2O_2, hydrogen peroxide; CdM, conditioned medium; hDF, human dermal fibroblast; hAEC, human amniotic epithelial cell; hAMSC, human amniotic mesenchymal stem cells; SOD, superoxide dismutase; CAT, catalase; MDA, malondialdehyde.

upregulated compared with the 200 μM H_2O_2 group (P<0.05; Fig. 5C and F). The ratio of γ-H2AX/H2AX is indicative of the phosphorylation level and 41.0±4.2, 476.0±8.5, 80.0±1.8 and 98.0±5.7% were determined for the control, the 200 μM H_2O_2, the CdM-hAEC and the CdM-hAMSC groups (Fig. 5G).

CdM from hAECs and hAMSCs reduces p21 and p16 expression in H_2O_2-induced premature senescence in hDFs. p21 and p16 are transcription factors and overexpression of p21 and p16 has previously shown to cause premature cell senescence (28). Expression of p21 and p16 was assessed by RT-qPCR and western blots. The results of RT-qPCR and western blot analysis showed that p21 and p16 expression was significantly upregulated in 200 μM H_2O_2-treated group compared with control untreated group (P<0.05; Fig. 5B-E). mRNA levels of p21 and protein levels of p21 and p16 were significantly reduced after CdM treatment when compared with the 200 μM H_2O_2 group (P<0.05; Fig. 5B-E).

Discussion

Stem cells derived from hAM have several advantages for beauty therapy, including that hAM is usually not utilized after delivery, small pieces of membrane can contain high levels of stem cells with easy expandability and hAM has low immunogenicity (29,30). These points provide favorable conditions for the application of hAM cells in cosmetic products.

In this study, effects of CdM-hAEC and CdM-hAMSC on H_2O_2-induced premature senescence in hDFs were examined. Previous reports have shown that hAMSCs protect against UVA irradiation-induced hDF senescence (31). The results of the presents study demonstrated that treatment with CdM reversed cellular senescence induced by H_2O_2. Cell proliferation and migration experiments were performed to evaluate effects of CdM on the biological function of hDFs. CdM promoted hDF proliferation in a dose-dependent manner and significantly promoted cell migration (24,32).

Oxidative and antioxidant systems co-exist in cells to maintain ROS balance, which may damage the cells, weaken cell function and result in premature cell senescence (33). SOD and CAT hydrolyze ROS and attenuate cell damage caused by free radicals, and MDA is an indicator of lipid peroxidation, which amplifies the ability of ROS to cause cell damage (34,35). Numerous studies have indicated that H_2O_2 increases the level of ROS in hDFs and attenuates the activity of antioxidant enzymes (36,37). In this study, it was discovered that using CdM after H_2O_2 treatment increased the activity of total-SOD and CAT, and decreased the levels of MDA and intercellular ROS in hDFs. Additionally, the oxidative stress-induced premature senescence phenotype was ameliorated by retaining the oxidation-reduction equilibrium.

Previous research has shown that activation of the DNA damage response (DDR) pathway is triggered by a continued high concentration of ROS (38). In case of failure to repair DSBs in time, this pathway activates the downstream signaling pathways, resulting in cell apoptosis or senescence (39). In addition, sustained DSB damage signals activate the ATM-Chk2-p53-p21-pRb and the p38-$p16^{INK4\alpha}$ signaling pathways (40), which maintain the cell senescence phenotype and block cell cycle progression (41). Results of the present study showed that a significant reduction in intracellular ROS after CdM treatment compared with the 200 μM H_2O_2 group. p21 and p16 inhibit cell cycle regulation by affecting the activity of various cyclin-dependent kinases, which eventually block the cell cycle (42). In addition, mRNA levels of p21 were also significantly reduced. 8-OHdG and γ-H2AX are sensitive damage markers of DSBs and both markers are commonly used to detect DNA base and nucleotide damage (43,44). H2AX is an important member of the H2A histone family. The H2A protein family includes H2A1-H2A2, H2AZ and H2AX. H2AX phosphorylation is a key step in the DDR, playing a role in signaling and initiating the repair of DSBs (45). H2AX phosphorylation creates an epigenetic signal that is recognized by specific domains on downstream DDR proteins. Accumulation of these proteins depends on H2AX phosphorylation but the accumulation rate can differ (46). The current study showed that H2AX phosphorylation increased in the presence of H_2O_2 and CdM reversed the observed phosphorylation potentially through enhanced dephosphorylation. One mechanism relies on the dephosphorylation of γ-H2AX by phosphatase 2A and phosphatase 4C (47,48). The other mechanism of γ-H2AX removal is through redistribution in the chromatin involving histone exchange and replacing γ-H2AX with H2AZ during chromatin remodeling, mediated by histone acetyltransferases (49,50). Previous studies suggested that transplanted AMSCs increase the activity of antioxidant enzymes and reduce DNA damage in a premature ageing model (51).

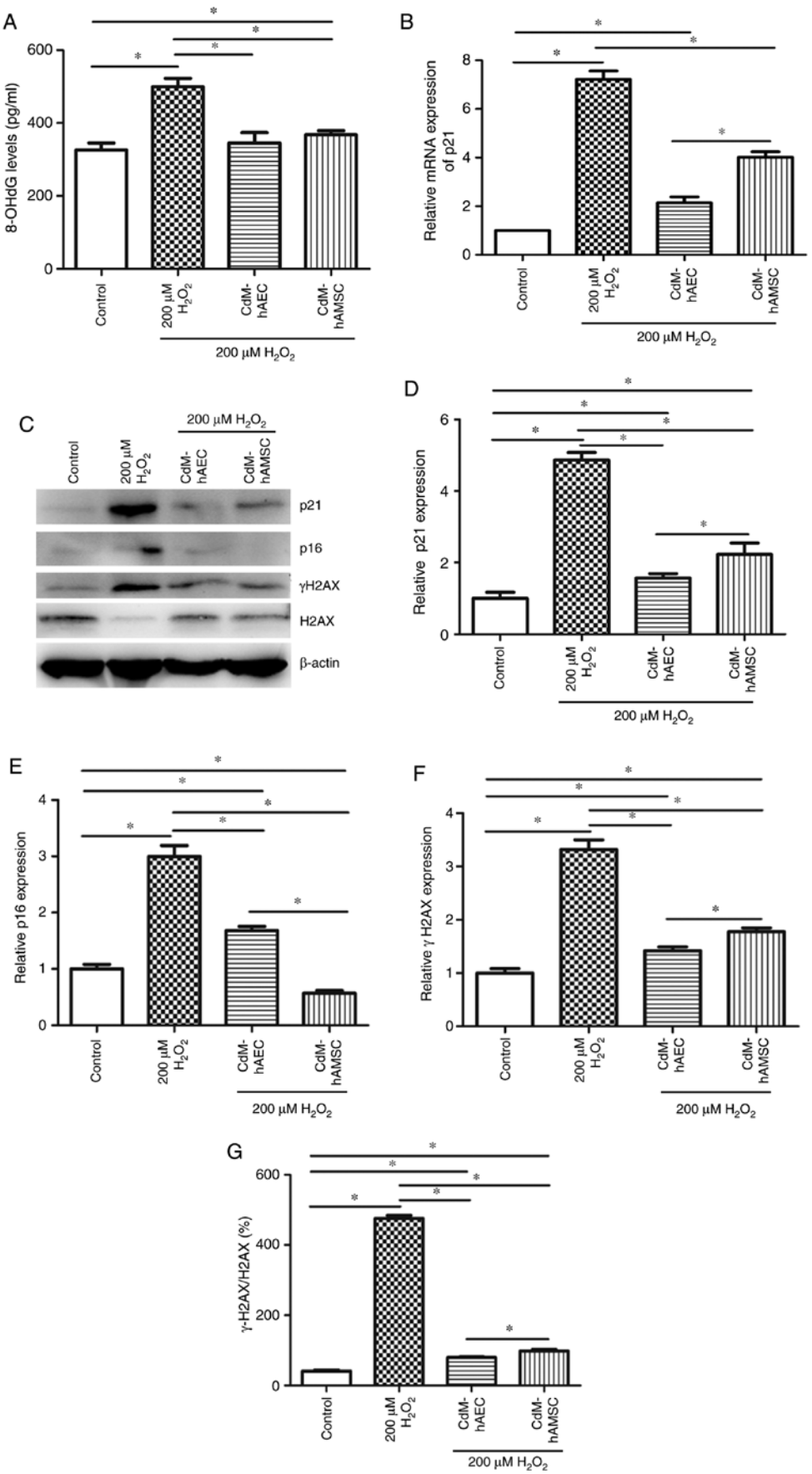

Figure 5. CdM affects DNA damage, and mRNA and protein expression in H_2O_2-treated hDFs. (A) 8-OHdG levels in hDFs measured using ELISA. (B) p21 mRNA expression determined by reverse transcription-quantitative PCR. (C) Western blot images and quantification of (D) p21, (E) p16, (F) γ-H2AX levels, as well as (G) the ratio of γ-H2AX to H2AX. β-actin was used as the internal control. Data are presented as the mean ± standard deviation (n=3). *P<0.05. H_2O_2, hydrogen peroxide; CdM, conditioned medium; hDF, human dermal fibroblast; hAEC, human amniotic epithelial cell; hAMSC, human amniotic mesenchymal stem cells; 8-OHdG, 8-hydroxydeoxyguanosine.

According to results of this study, CdM alleviated DNA damage caused by hydrogen peroxide. Therefore, CdM may delay aging caused by oxidative stress in cells.

In conclusion, utilizing CdM was a novel cell-free treatment strategy for potential anti-aging applications, supported by evidence indicating that healing effects of stem cells are associated with their paracrine properties (52). The extraction of secretory proteins from the CdM from adipose stem cells has previously been injected into human skin for facial anti-aging (53). CdM from hAECs and hAMSCs used here contained various growth factors, cytokines and proteins that improved cell function. Other reports have shown that hAM cells promote senescent hDF function (31). However, little is known about the components in the CdM that make it resistant to damage from H_2O_2 and delay cell aging. Future work may concern high-throughput sequencing of hAM derived cells coupled to simultaneous mass spectrometry analyses of the CdM to identify differentially expressed proteins. The present results demonstrated that CdM-hAEC and CdM-hAMSC delayed H_2O_2-induced premature senescence of hDFs and the CdM potentially can be applied in the field of anti-aging.

Acknowledgements

Not applicable.

Funding

This study was supported by the Shenyang Key R&D and Technology Transfer Program (grant no. 250039).

Availability of data and materials

All data generated or analyzed during this study are included in this published article.

Authors' contributions

XP and FZ conceived and designed the experiments. HL contributed to hAMSC, hDF and hAEC collection. HL, TZ, RW, XL and PS contributed reagents, materials and the analysis of the data. CP performed experiments and prepared the manuscript. All authors read and approved the final manuscript.

Ethics approval and consent to participate

The present study was approved by the Ethics Committee of the First Affiliated Hospital and Shengjing Hospital of China Medical University (Shenyang, China). Written informed consent was obtained from all patients.

Patient consent for publications

Not applicable.

Competing interests

The authors declare that they have no competing interests.

References

1. Varani J: Fibroblast aging: Intrinsic and extrinsic factors. Drug Discov Today Ther Strateg 7: 65-70, 2010.
2. Makrantonaki E and Zouboulis CC: Molecular mechanisms of skin aging: State of the art. Ann N Y Acad Sci 1119: 40-50, 2007.
3. Seo MY, Chung SY, Choi WK, Seo YK, Jung SH, Park JM, Seo MJ, Park JK, Kim JW and Park CS: Anti-aging effect of rice wine in cultured human fibroblasts and keratinocytes. J Biosci Bioeng 107: 266-271, 2009.
4. Marcotte R and Wang E: Replicative senescence revisited. J Gerontol A Biol Sci Med Sci 57: B257-B269, 2002.
5. Serrano M and Blasco MA: Putting the stress on senescence. Curr Opin Cell Biol 13: 748-753, 2001.
6. Chen QM: Replicative senescence and oxidant-induced premature senescence. Beyond the control of cell cycle checkpoints. Ann N Y Acad Sci 908: 111-125, 2000.
7. Cheng H, Qiu L, Ma J, Zhang H, Cheng M, Li W, Zhao X and Liu K: Replicative senescence of human bone marrow and umbilical cord derived mesenchymal stem cells and their differentiation to adipocytes and osteoblasts. Mol Biol Rep 38: 5161-5168, 2011.
8. Jiang B, Li Y, Liang P, Liu Y, Huang X, Tong Z, Zhang P, Huang X, Liu Y and Liu Z: Nucleolin enhances the proliferation and migration of heat-denatured human dermal fibroblasts. Wound Repair Regen 23: 807-818, 2015.
9. Feng B, Fang Y and Wei SM: Effect and mechanism of epigallocatechin-3-gallate (EGCG). Against the hydrogen peroxide-induced oxidative damage in human dermal fibroblasts. J Cosmet Sci 64: 35-44, 2013.
10. Hernández-García D, Wood CD, Castro-Obregón S and Covarrubias L: Reactive oxygen species: A radical role in development? Free Radic Biol Med 49: 130-143, 2010.
11. Halliwell B and Gutteridge JMC: Free radicals in biology and medicine. J Free Radic Biol Med 1: 331-332, 2007.
12. Gutteridge JMC and Halliwell B: Mini-review: Oxidative stress, redox stress or redox success? Biochem Biophys Res Commun 502: 183-186, 2018.
13. Ames BN, Shigenaga MK and Hagen TM: Oxidants, antioxidants, and the degenerative diseases of aging. Proc Natl Acad Sci USA 90: 7915-7922, 1993.
14. Djamali A: Oxidative stress as a common pathway to chronic tubulointerstitial injury in kidney allografts. Am J Physiol Renal Physiol 293: F445-F455, 2007.
15. Van Deursen JM: The role of senescent cells in ageing. Nature 509: 439-446, 2014.
16. Harman D: The biologic clock: The mitochondria. J Am Geriatr Soc 20: 145-147, 1972.
17. Díaz-Prado S, Muiños-López E, Hermida-Gómez T, Rendal-Vázquez ME, Fuentes-Boquete I, de Toro FJ and Blanco FJ: Multilineage differentiation potential of cells isolated from the human amniotic membrane. J Cell Biochem 111: 846-857, 2010.
18. Castellanos G, Bernabé-García Á, Moraleda JM and Nicolás FJ: Amniotic membrane application for the healing of chronic wounds and ulcers. Placenta 59: 146-153, 2017.
19. Zhao B, Liu JQ, Zheng Z, Zhang J, Wang SY, Han SC, Zhou Q, Guan H, Li C, Su LL and Hu DH: Human amniotic epithelial stem cells promote wound healing by facilitating migration and proliferation of keratinocytes via ERK, JNK and AKT signaling pathways. Cell Tissue Res 365: 85-99, 2016.
20. Hahn HJ, Kim KB, An IS, Ahn KJ and Han HJ: Protective effects of rosmarinic acid against hydrogen peroxide-induced cellular senescence and the inflammatory response in normal human dermal fibroblasts. Mol Med Rep 16: 9763-9769, 2017.
21. Abdul Hisam EE, Rofiee MS, Khalid AM, Jalaluddin AF, Mohamad Yusof MI, Idris MH, Ramli S, James RJ, Jack Yoeng W, Lay Kek T and Salleh MZ: Combined extract of Moringa oleifera and Centella asiatica modulates oxidative stress and senescence in hydrogen peroxide-induced human dermal fibroblasts. Turk J Biol 42: 33-44, 2018.
22. Borodkina A, Shatrova A, Abushik P, Nikolsky N and Burova E: Interaction between ROS dependent DNA damage, mitochondria and p38MAPK underlies senescence of human adult stem cells. Aging (Albany NY) 6: 481-495, 2014.
23. Priya D, Selokar NL, Raja AK, Saini M, Sahare AA, Nala N, Palta P, Chauhan MS, Manik RS and Singla SK: Production of wild buffalo (Bubalus arnee) embryos by interspecies somatic cell nuclear transfer using domestic buffalo (Bubalus bubalis) oocytes. Reprod Domest Anim 49: 343-351, 2014.

24. Liu X, Wang Z, Wang R, Zhao F, Shi P, Jiang Y and Pang X: Direct comparison of the potency of human mesenchymal stem cells derived from amnion tissue, bone marrow and adipose tissue at inducing dermal fibroblast responses to cutaneous wounds. Int J Mol Med 31: 407-415, 2013.
25. Wang G, Zhao F, Yang D, Wang J, Qiu L and Pang X: Human amniotic epithelial cells regulate osteoblast differentiation through the secretion of TGFβ1 and microRNA-34a-5p. Int J Mol Med 41: 791-799, 2018.
26. Flach J, Bakker ST, Mohrin M, Conroy PC, Pietras EM, Reynaud D, Alvarez S, Diolaiti ME, Ugarte F, Forsberg EC, *et al*: Replication stress is a potent driver of functional decline in ageing haematopoietic stem cells. Nature 512: 198-202, 2014.
27. Sperka T, Wang J and Rudolph KL: DNA damage checkpoints in stem cells, ageing and cancer. Nat Rev Mol Cell Biol 13: 579-590, 2012.
28. Zhou L, Chen X, Liu T, Gong Y, Chen S, Pan G, Cui W, Luo ZP, Pei M, Yang H and He F: Melatonin reverses H_2O_2-induced premature senescence in mesenchymal stem cells via the SIRT1-dependent pathway. J Pineal Res 59: 190-205, 2015.
29. Díaz-Prado S, Muiños-López E, Hermida-Gómez T, Rendal-Vázquez ME, Fuentes-Boquete I, de Toro FJ and Blanco FJ: Multilineage differentiation potential of cells isolated from the human amniotic membrane. J Cell Biochem 111: 846-857, 2010.
30. Kim EY, Lee KB and Kim MK: The potential of mesenchymal stem cells derived from amniotic membrane and amniotic fluid for neuronal regenerative therapy. BMB Rep 47: 135-140, 2014.
31. Zhang C, Yuchi H, Sun L, Zhou X and Lin J: Human amnion-derived mesenchymal stem cells protect against UVA irradiation-induced human dermal fibroblast senescence, in vitro. Mol Med Rep 16: 2016-2022, 2017.
32. Kim WS, Park BS, Sung JH, Yang JM, Park SB, Kwak SJ and Park JS: Wound healing effect of adipose-derived stem cells: A critical role of secretory factors on human dermal fibroblasts. J Dermatol Sci 48: 15-24, 2007.
33. Xiao H, Xiong L, Song X, Jin P, Chen L, Chen X, Yao H, Wang Y and Wang L: Angelica sinensis polysaccharides ameliorate stress-induced premature senescence of hematopoietic cell via protecting bone marrow stromal cells from oxidative injuries caused by 5-fluorouracil. Int J Mol Sci 18: pii E2265, 2017.
34. Faraci FM and Didion SP: Vascular protection: Superoxide dismutase isoforms in the vessel wall. Arterioscler Thromb Vasc Biol 24: 1367-1373, 2004.
35. Jin J, Lv X, Chen L, Zhang W, Li J, Wang Q, Wang R, Lu X and Miao D: Bmi-1 plays a critical role in protection from renal tubulointerstitial injury by maintaining redox balance. Aging Cell 13: 797-809, 2014.
36. Park MJ and Bae YS: Fermented acanthopanax koreanum root extract reduces UVB- and H2O2-induced senescence in human skin fibroblast cells. J Microbiol Biotechnol 26: 1224-1233, 2016.
37. Choi SI, Lee JH, Kim JM, Jung TD, Cho BY, Choi SH, Lee DW, Kim J, Kim JY and Lee OH: Ulmus macrocarpa hance extracts attenuated H_2O_2 and UVB-Induced skin photo-aging by activating antioxidant enzymes and inhibiting MAPK pathways. Int J Mol Sci 18: pii E1200, 2017.
38. Lombard DB, Chua KF, Mostoslavsky R, Franco S, Gostissa M and Alt FW: DNA repair, genome stability, and aging. Cell 120: 497-512, 2005.
39. Kuilman T, Michaloglou C, Mooi WJ and Peeper DS: The essence of senescence. Genes Dev 24: 2463-2479, 2010.
40. Boyette LB and Tuan RS: Adult stem cells and diseases of aging. J Clin Med 3: 88-134, 2014.
41. Bockeria L, Bogin V, Bockeria O, Le T, Alekyan B, Woods EJ, Brown AA, Ichim TE and Patel AN: Endometrial regenerative cells for treatment of heart failure: A new stem cell enters the clinic. J Transl Med 11: 56, 2013.
42. Savickienė J, Baronaitė S, Zentelytė A, Treigytė G and Navakauskienė R: Senescence-associated molecular and epigenetic alterations in mesenchymal stem cell cultures from amniotic fluid of normal and fetus-affected pregnancy. Stem Cells Int 2016: 2019498, 2016.
43. Kasai H and Nishimura S: Hydroxylation of deoxyguanosine at the C-8 position by ascorbic acid and other reducing agents. Nucleic Acids Res 12: 2137-2145, 1984.
44. Rodier F and Campisi J: Four faces of cellular senescence. J Cell Biol 192: 547-556, 2011.
45. Mah LJ, El-Osta A and Karagiannis TC: gammaH2AX: A sensitive molecular marker of DNA damage and repair. Leukemia 4: 679-686, 2010.
46. Bhogal N, Jalali F and Bristow RG: Microscopic imaging of DNA repair foci in irradiated normal tissues. Int J Radiat Biol 9: 732-746, 2009.
47. Downs JA, Allard S, Jobin-Robitaille O, Javaheri A, Auger A, Bouchard N, Kron SJ, Jackson SP and Côté J: Binding of chromatin-modifying activities to phosphorylated histone H2A at DNA damage sites. Mol Cell 6: 979-990, 2004.
48. Ikura T, Tashiro S, Kakino A, Shima H, Jacob N, Amunugama R, Yoder K, Izumi S, Kuraoka I, Tanaka K, *et al*: DNA damage-dependent acetylation and ubiquitination of H2AX enhances chromatin dynamics. Mol Cell Biol 20: 7028-7040, 2007.
49. Altaf M, Auger A, Covic M and Côté J: Connection between histone H2A variants and chromatin remodeling complexes. Biochem Cell Biol 1: 35-50, 2009.
50. Kusch T, Florens L, Macdonald WH, Swanson SK, Glaser RL, Yates JR, Abmayr SM, Washburn MP and Workman JL: Acetylation by Tip60 is required for selective histone variant exchange at DNA lesions. Science 306: 2084-2087, 2004.
51. Xie C, Jin J, Lv X, Tao J, Wang R and Miao D: Anti-aging effect of transplanted amniotic membrane mesenchymal stem cells in a premature aging model of Bmi-1 deficiency. Sci Rep 5: 13975, 2015.
52. Li F and Zhao SZ: Mesenchymal stem cells: Potential role in corneal wound repair and transplantation. World J Stem Cells 6: 296-304, 2014.
53. Xu Y, Guo S, Wei C, Li H, Chen L, Yin C and Zhang C: The comparison of adipose stem cell and placental stem cell in secretion characteristics and in facial antiaging. Stem Cells Int 2016: 7315830, 2016.